Cluster-folding analysis of $^6\vec{\text{Li}}$ +^{26}Mg scattering at 60 MeV

K. Rusek,* N. M. Clarke, and R. P. Ward

School of Physics and Space Research, University of Birmingham, Edgbaston, Birmingham B15 2TT, England
(Received 22 June 1994)

Data for the elastic and inelastic scattering of 60 MeV polarized ^{6}Li by ^{26}Mg have been analyzed using coupled-channels (CC) techniques. The diagonal and off-diagonal interaction potentials used in the analysis were derived from empirical $\alpha+^{26}$Mg and $d+^{26}$Mg optical model potentials by means of the cluster-folding method. The effects of projectile excitation to the three low-lying $T = 0$ resonant states, as well as to nonresonant continuum states ranging from 2.1 MeV to 11.5 MeV excitation energy relative to the ^{6}Li ground state, have also been studied. A good description of the data has been achieved without renormalization of the interaction potentials.

I. INTRODUCTION

Since the first demonstration by Thompson and Nagarajan [1] it has been widely recognized that the breakup of ^{6}Li into $\alpha + d$ plays a crucial role in the elastic scattering of ^{6}Li from a range of target nuclei and at different energies. Tensor analyzing powers (TAP's) of the first- and second-rank measured in experiments with polarized lithium beams are known to be especially sensitive to such breakup effects, which are generally spin dependent [2]. To account for breakup effects, data for ^{6}Li elastic scattering are usually analyzed by coupled-channels (CC) calculations with interaction potentials derived either from nucleon-nucleon forces by the double-folding (DF) method [3] or from α-target and d-target phenomenological potentials using a single-folding procedure. The latter is based on the $\alpha + d$ cluster model of ^{6}Li and is known as the cluster-folding (CF) method [4].

The scattering system $^6\vec{\text{Li}}$ +^{26}Mg has been thoroughly investigated. Data for polarized ^{6}Li scattering from ^{26}Mg at 44 MeV [5], containing the full set of TAP's, have been analyzed a number of times [5–8] using both DF and CF techniques. The conclusions of these analyses can be summarized as follows.

(1) The elastic differential cross section is well described by CC calculations with DF potentials, including the effects of the first three resonant $T = 0$ excited states of ^{6}Li as well as $\alpha + d$ nonresonant continuum states up to an excitation energy of approximately 22.6 MeV [7]. When the CF interaction is used, however, CC calculations fail to reproduce the differential cross section without a substantial reduction of the real CF potential strength [6]. Although the origin of this renormalization is unknown, it is expected that the need for it may vanish at the higher incident energy.

(2) The description of the TAP's by CC calculations

with DF potentials is rather poor [7]. Generally, such calculations predict much larger values for the TAP's than calculations with CF potentials [8] which more accurately reproduce the data.

(3) The role of the spin-orbit potential in the description of the first rank TAP is found to be negligible in comparison with dynamic effects due to couplings to the $\alpha + d$ breakup channels [8]. Moreover, the effects of the couplings on the second-rank TAP's are reported to be very large [8], which puts into question the feasibility of studying the ^{6}Li-target second-rank tensor potential using polarized ^{6}Li beams [4,9,10]. It should be noted that Hirabayashi and Sakuragi did not use a second-rank tensor potential for the elastic channel in their analysis [8].

One may surmise that the success in the description of the differential cross section for ^{6}Li +^{26}Mg elastic scattering by CC calculations with DF potentials, in contrast with the rather poor description of the TAP's, stems from unrealistic strengths for the coupling potentials emerging from the DF calculations. Thus, a study similar to that of Hirabayashi [7], but with the coupling potentials calculated by means of the CF method, would be of particular interest [8].

Recently, data on polarized ^{6}Li elastic and inelastic scattering from ^{26}Mg became available at 60 MeV bombarding energy [11]. In the present paper the results are reported of a CC analysis of this new data. The analysis is based on the $\alpha + d$ cluster model of ^{6}Li, with all the central and coupling potentials calculated by means of the CF method [4]. The effects of $T = 0$ resonant as well as nonresonant continuum excited states of ^{6}Li are taken into account. The aim of this analysis is to compare the results with the results of a similar analysis using DF potentials at 44 MeV [7].

II. ANALYSIS

The CC calculations were performed using version FRW of the coupled-channels computer code FRESCO [12], which allows a treatment [13] of the

---

*Present address: Soltan Institute for Nuclear Studies, Zaklad 1, Hoza 69, 00 681 Warsaw, Poland.

unbound states of the ^{6}Li $= \alpha + d$ system similar to the continuum-discretized coupled-channels (CDCC) method [14,15]. The $\alpha + d$ continuum above the ^{6}Li breakup threshold was discretized into a set of momentum bins with respect to the momentum $\hbar k$ of the α–d relative motion, where

$$k^2 = \frac{2\mu}{\hbar^2} E_x \ . \tag{1}$$

The quantity E_x is the ^{6}Li excitation energy above the $\alpha + d$ breakup threshold and μ is the reduced mass of the $\alpha + d$ cluster system. The cluster wave functions $\psi(r, k)$ in a bin were averaged over the bin width Δk and normalized to unity according to [13]

$$\Psi(r) = \frac{1}{\sqrt{N}} \int_{\Delta k} \psi(r, k)\, dk \ , \tag{2}$$

$$\langle \Psi(r) \mid \Psi(r) \rangle = 1 \ , \tag{3}$$

where N is a normalization factor and r is the α–d separation. Each bin was then treated as an excited state of ^{6}Li represented by a wave function $\Psi(r)$ at an energy corresponding to the mean energy of the bin and having spin $\vec{I}$ and parity $(-1)^L$. The angular momenta $\vec{I}$ and $\vec{L}$ are related by $\vec{I} = \vec{L} + \vec{s}$, where $\vec{s}$ is the spin of the deuteron cluster and $\vec{L}$ is the relative angular momentum of $\alpha + d$ cluster system. Following Hirabayashi [7], L was limited to the values $0, 1, 2$.

The ground state of ^{6}Li was assumed to be a pure $L = 0$ $\alpha + d$ cluster state with a radial wave function calculated in a potential well having a Woods-Saxon shape and the geometry parameters $R = 1.9$ fm and $a_0 = 0.65$ fm [16]. The depth of this binding potential was varied in order to reproduce the binding energy of 1.474 MeV.

The three $L = 2$ resonant states at excitation energies 2.19, 4.31, and 5.65 MeV, having spins $3^+, 2^+$, and 1^+ [17], respectively, were treated using the so-called weak binding-energy approximation (WBEA). The validity of this approximation was confirmed for polarized ^{6}Li scattering from ^{26}Mg at 44 MeV [8]. The first 3^+ state was approximated by a bound state having a very small binding energy. The binding potential had a similar shape and geometry as that of the $L = 0$ ground state with a depth adjusted in order to reproduce this small binding energy. The radial wave functions of the 2^+ and 1^+ states were assumed to be identical to that for the 3^+ state.

A. Optical potentials

CF calculations for $^6\vec{\text{Li}} + {}^{26}$Mg scattering at 60 MeV require $\alpha + {}^{26}$Mg and $\vec{d} + {}^{26}$Mg phenomenological optical potentials derived from 40 MeV and 20 MeV data, respectively. However, the choice of these parameters is often a source of difficulty because of the presence of ambiguities [8]. Singh et al., in their study of α-particle scattering from ^{24}Mg at 40 MeV, reported two sets of parameters (denoted set A and set B) which gave equivalent

fits to their data [18]. The elastic scattering of polarized deuterons from ^{26}Mg at 20 MeV bombarding energy has not been investigated, although a 52 MeV study was performed by Nurzynski et al. [19]. However, global analyses of deuteron scattering have been performed by Lohr and Haeberli [20] and Daehnick et al. [21]. In their study of polarized deuteron scattering from ^{24}Mg at 20 MeV, Clement et al. [22] found that calculations performed with the global parameter sets of Lohr and Haeberli and Daehnick et al. gave essentially the same results.

CF calculations were performed using set A derived by Singh et al. for the α-target interaction in conjunction with the d-target global parameter set of Lohr and Haeberli and set L of Daehnick et al. The real parts of the CF central potential for ^{6}Li $+ {}^{26}$Mg calculated using the two d-target sets are very similar at projectile-target separations of 7–8 fm, the range important for this scattering. However, the imaginary part of the potential calculated using the deuteron set of Lohr and Haeberli is almost two times larger than that calculated using the set of Daehnick et al. The largest difference, however, is seen for the ^{6}Li $+ {}^{26}$Mg CF spin-orbit potential. The spin-orbit potential derived from the deuteron set of Daehnick et al. is nearly ten times larger at the separations important for the scattering than the potential derived from the set of Lohr and Haeberli.

The results of the CC calculations shown in Figs. 1–5 were obtained with central CF potentials for $^6\vec{\text{Li}} + {}^{26}$Mg derived from the deuteron set of Daehnick et al. and set A of Singh et al. The CF spin-orbit potential, however, was derived from the deuteron spin-orbit potential parameters reported by Lohr and Haeberli; these parameters were also used in the analysis of Hirabayashi and Sakuragi [8]. Since the second-rank tensor potential T_R for the $\vec{d} + {}^{26}$Mg scattering system has not been investigated, the tensor interaction between ^{6}Li and ^{26}Mg was omitted in the present analysis.

B. Test calculations

First, the limitation of the momentum space $\hbar k$ was studied for the nonresonant ^{6}Li excited states. An important conclusion of the study performed by Hirabayashi [7] was that full CDCC calculations for the nonresonant states can be reasonably approximated by calculations with the value of the relative angular momentum L limited to zero. With this in mind, we examined the convergence of the calculated results with respect to the size of the momentum space with the nonresonant states limited to those with $L = 0$ only. The results are plotted in Fig. 1. The results of CC calculations which include couplings to the three $T = 0$ resonant excited states of ^{6}Li only are shown by dashed curves. The $L = 0$ nonresonant continuum states were divided into three $\Delta k = 0.2$ fm^{-1} bins, ranging from $k_{\text{min}} = 0.2$ fm^{-1} to $k_{\text{max}} = 0.8$ fm^{-1}; the inclusion of these states seriously affected the predictions, reducing the differential cross section for ^{6}Li $+ {}^{26}$Mg elastic scattering and shifting the oscillations to more backward angles. The oscillations of the predicted first-rank TAP were also shifted to more

backward angles. Increasing the value of k_{max} to 1.0 fm^{-1} changed these results only slightly. Similarly, reducing the value of k_{min} to 0.05 fm^{-1} did not affect the results considerably. Thus, limiting the model momentum space to $0.2 \le k \le 0.8$ fm^{-1}, corresponding to a ^{6}Li excitation energy range of $2.1 \le E_x \le 11.5$ MeV relative to the ^{6}Li ground state, seems to be a reasonable approximation for the present purpose. A very careful examination of the k limits for ^{6}Li $+^{26}$Mg scattering at 99 MeV bombarding energy lead to the conclusion that the upper limit k_{max} at this energy should not be smaller than 1.2 fm^{-1}, while k_{min} can indeed be set to 0.2 fm^{-1} [7]. The radius R_{max} limiting the range of the wave functions in the calculations was set to 30.0 fm. Calculations with $R_{max} = 60$ fm were found to yield essentially the same results.

As a next step we studied how the calculated results depend on the bin width Δk. CC calculations including the three $T = 0$ resonant states and the $L = 0$ nonresonant continuum states of ^{6}Li within limits $0.2 \le k \le 0.8$ fm^{-1} were performed with Δk ranging from 0.05 to 0.6 fm^{-1}. It was found that setting the bin width to 0.2 fm^{-1} was sufficient for the present purpose. We noted, however, that the results of calculations with
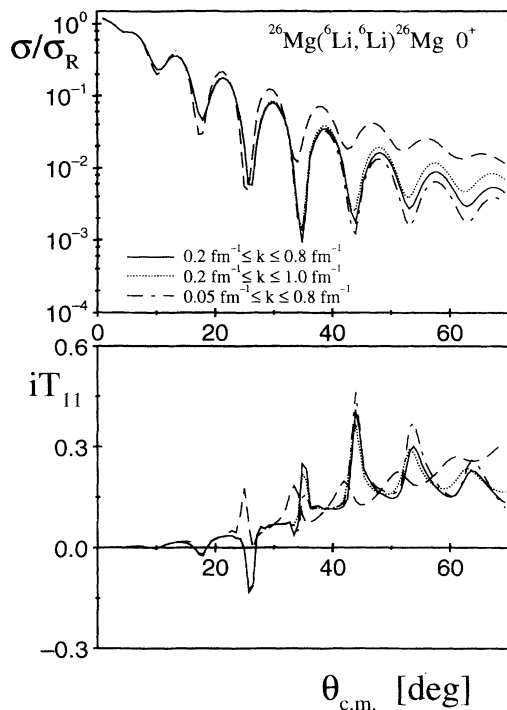

FIG. 1. Angular distributions of differential cross section and first-rank TAP for ^{6}Li $+^{26}$Mg elastic scattering at 60 MeV. The solid, dotted, and dot-dashed curves represent the results of CC calculations including the three low-lying $L = 2$ ($I^\pi = 3^+, 2^+, 1^+$) resonant $\alpha + d$ states of ^{6}Li and $L = 0$ ($I^\pi = 1^+$) nonresonant continuum states within the α-d relative momentum range $\hbar k$ indicated in the figure. The momentum space was divided into three bins in each case. The dashed curves correspond to four-channel calculations including the ground state and the $L = 2$ resonant states only.
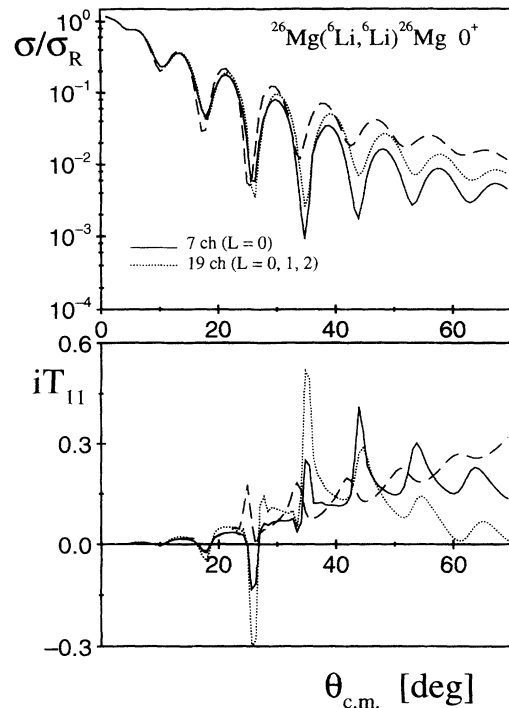

FIG. 2. Angular distributions of differential cross section and first-rank TAP for ^{6}Li $+^{26}$Mg elastic scattering at 60 MeV. The solid and dashed curves are as in Fig. 1, while the dotted curves represent the results of CC calculations with the momentum space divided into $L = 0, 1, 2$ nonresonant $\alpha + d$ continuum states.

$\Delta k = 0.3$ fm^{-1} did not differ significantly from those with $\Delta k = 0.2$ fm^{-1}. The calculated angular distributions of the differential cross section within the angular range $0° \le \theta_{c.m.} \le 70°$ are almost undistinguishable for these two cases, although some differences are seen for the first-rank TAP's.

The detailed calculations performed by Hirabayashi for ^{6}Li $+^{26}$Mg elastic scattering at 99 MeV [7] suggested that, due to a cancellation between the contributions from the $L = 1$ and $L = 2$ nonresonant states, CC calculations which include only $L = 0$ nonresonant states (in addition to the $L = 2$ resonant states) are a good approximation to full CDCC calculations. To study this cancellation at the lower energy of 60 MeV CC calculations were performed with the $\hbar k$ space divided in line with [7]. The upper limit of k, however, was set to 0.8 fm^{-1} as discussed previously. The width of each bin was set in accordance with reference [7] to 0.2 fm^{-1}. In these CC calculations we included $L = 0, 1, 2$ nonresonant continuum states within the limits $0.2 \le k \le 0.8$ fm^{-1}. The model space $\hbar k$ for $L = 2$ nonresonant continuum states was different for each spin I. States with $I^\pi = 3^+$ were considered within limits $0.4 \le k \le 0.8$ fm^{-1}, while for $I^\pi = 2^+$ states the limits were set to $0.6 \le k \le 0.8$ fm^{-1}. For $I^\pi = 1^+$ only the resonant state at an excitation energy of 5.65 MeV was assumed. The results of the calculations are plotted in Fig. 2. As in Fig. 1 the results of four-channel calculations, including cou-

plings to the three $T = 0$ resonant excited states only, are shown as a dashed line. The comparison of CC calculations with the nonresonant excited states limited to those with $L = 0$ (seven-channel calculations) and with $L = 0, 1, 2$ (19-channel calculations) reveals some similarities with the calculations performed by Hirabayashi [7]. The differential cross section for elastic scattering calculated with the inclusion of the $L = 0, 1, 2$ nonresonant continuum states is larger than that calculated with the inclusion of the $L = 0$ states only. Moreover the inclusion of the $L = 1, 2$ nonresonant continuum states shifts the oscillations of both the angular distributions only very slightly. However, the amplitude of the oscillations in the predicted first-rank TAP is reduced at scattering angles larger then 40°, while the calculations of Hirabayashi exhibit exactly the opposite effect.

C. Analysis of elastic and inelastic scattering

Excitation of the target to the first excited 2^+ state at 1.81 MeV was found previously [5] to play only a minor role in the elastic scattering of ^{6}Li from ^{26}Mg. In this
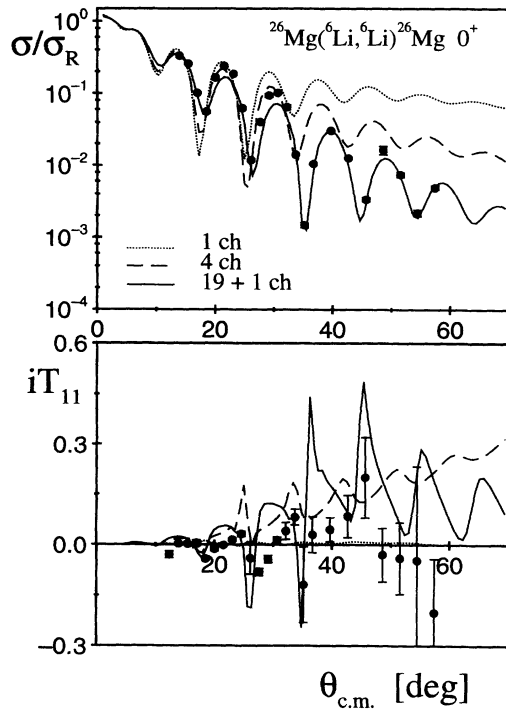
FIG. 3. Data for ^{6}Li $+^{26}$Mg elastic scattering at 60 MeV compared with the results of CC calculations. The dotted curves correspond to one-channel calculations without projectile or target excitations. The dashed curves have the same meaning as in Figs. 1 and 2, while the solid curves represent the results of calculations including excitation of ^{6}Li to the three $L = 2$ resonant $\alpha + d$ states as well as $L = 0, 1, 2$ $\alpha + d$ nonresonant continuum states as in Fig. 2 and the excitation of ^{26}Mg to its first 2^+ excited state at 1.81 MeV. The diagonal and coupling potentials derived by means of the CF method have not been renormalized in the course of calculations.
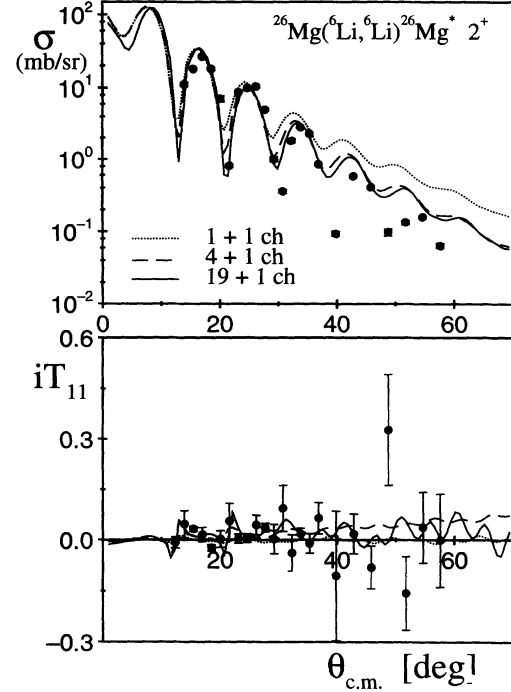
FIG. 4. Data for ^{6}Li $+^{26}$Mg inelastic scattering at 60 MeV populating the first excited state of ^{26}Mg. The dotted curves correspond to calculations without projectile excitations. The dashed curves represent the results of calculations including excitations of ^{6}Li to the three $L = 2$ resonant states as well as the target excitation. The solid curves have the same meaning as in Fig. 3.

work we included it in the analysis in a similar way to that used in [5]. The transition potential between the ground and first excited states of ^{26}Mg was calculated assuming a simple rotational model of ^{26}Mg [23]. The deformation lengths for the real and imaginary parts of the transition potential were assumed to be equal; their value

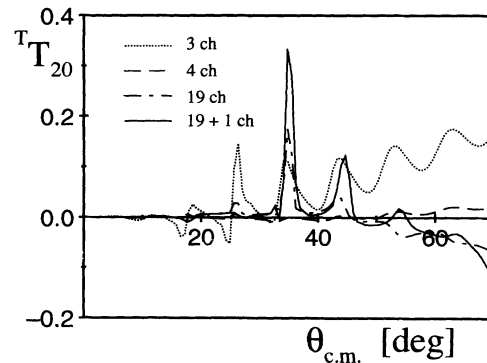FIG. 5. Predicted angular distribution of the second-rank TAP for elastic scattering of ^{6}Li $+^{26}$Mg at 60 MeV. The dotted and dashed curves represent the results of CC calculations with the two $I^\pi = 3^+, 2^+$ and all three $L = 2$ resonant excited states of ^{6}Li included, respectively. The solid and dot-dashed curves correspond to calculations including the three $L = 2$ resonant states as well as nonresonant continuum states of ^{6}Li as in Fig. 2 with and without excitation of the target, respectively.

of 1.25 fm was adopted from the lower energy study [5].

In Fig. 3 the results of calculations are compared with the experimental data for ^{6}Li $+^{26}$Mg elastic scattering. The one-channel or optical model calculations with a CF diagonal potential comprised of central and spin-orbit parts overestimated the differential cross section data, as shown by the dotted curve. To reproduce the differential cross section data with a one-channel calculation, the real part of the central CF potential had to be multiplied by a factor of 0.5 and the imaginary part by 1.5. Moreover the calculations predicted values of the first-rank TAP iT_{11} which were much smaller than the data.

Four-channel calculations, including projectile excitation to the three $L = 2$ resonant states, reduced significantly the farside component of the scattering amplitude, while the nearside component was almost unchanged. This resulted in a reduction of the calculated values of the differential cross section and a shift of the angular distribution oscillations to more backward angles. The four-channel calculations significantly modified the predictions for the first-rank TAP. Although the description of the experimental data was generally improved, the calculations still overpredicted the elastic scattering differential cross section data. Under these circumstances a need existed for a reduction of the real part of the central CF potential by about 35% in order to obtain a reasonable reproduction of the data.

The inclusion of coupling to $\alpha + d$ nonresonant continuum states of ^{6}Li corresponding to the excitation energy range from 2.1 to 11.5 MeV and intercluster relative angular momentum $L = 0, 1, 2$ shifted the oscillations of the differential cross section angular distribution so that their positions agreed with the oscillations measured in the experiment. It reduced further the values of the differential cross section too, as seen from the comparison of the dashed and dotted curves in Fig. 2, and changed significantly the angular distribution of the first-rank TAP.

Excitation of the target nucleus to the first excited state at 1.81 MeV produced an effect equivalent to the imaginary part of the central potential, in that it reduced the values of the elastic scattering differential cross section but did not shift the position of the oscillations. The final 20-channel calculations, including projectile and target excitations, yielded a good description of both angular distributions measured in the elastic channel, as shown by solid curves in Fig. 3.

The full 20-channel calculations also reproduced well the data in the inelastic channel, corresponding to the excitation of ^{26}Mg to its 2^+ first excited state, as shown in Fig. 4. The difference between these calculations and the calculations including excitation of ^{6}Li to the three $L = 2$ resonant states (five-channel, dashed curves in Fig. 4) is not as distinct as it was in the elastic channel. Thus, coupling to nonresonant states plays a role in the inelastic channel, but this role is not as important as that observed in the elastic scattering.

Projectile excitation to the resonant and nonresonant $\alpha + d$ states generated large values of the first-rank TAP in the elastic channel. It affected also the second-rank TAP as presented in Fig. 5. In the CC calculations the second-rank tensor potential for the $^6\vec{\text{Li}} +^{26}$Mg elastic channel was not included, therefore the results plotted in Fig. 5 are entirely due to projectile excitation. Coupling to the first two $L = 2$ ($I^\pi = 3^+, 2^+$) resonant excited states of ^{6}Li produced a substantial effect on $^TT_{20}$ (three-channel calculations in Fig. 5). It is, however, almost completely cancelled out by the inclusion of the third $L = 2$ ($I^\pi = 1^+$) resonant state. A similar cancellation has been observed in CC calculations with CF potentials performed for $^6\vec{\text{Li}} +^{120}$ Sn scattering at 44 MeV [8,10]. The nonresonant continuum states again enhanced the second-rank TAP, which was then amplified by the inclusion of target excitation. It is worthwhile to note that the inclusion of the nonresonant states shifted the oscillations in the $^TT_{20}$ angular distribution only slightly. The peaks produced by three-channel calculations at scattering angles of approximately $34°, 44°$, and $53°$ remain at almost the same angular positions in the 20-channel calculations. This is in contrast to the effect observed for the first-rank TAP.

III. DISCUSSION AND SUMMARY

The analysis of polarized ^{6}Li scattering from ^{26}Mg at 60 MeV by CC calculations with CF potentials led to a good description of the differential cross section and first-rank TAP data for elastic and inelastic scattering. These calculations fit the experimental data better, especially for the TAP in the elastic channel, than CC calculations with DF potentials performed at the lower energy of 44 MeV [7]. The analysis was parameter-free since all the input parameters, including the deformation lengths scaling the coupling potentials for the target excitation, were based on previous studies. Moreover, the analysis was free of any artificial factors, for example the renormalization factors N_r and N_i commonly used to vary the strengths of the real and imaginary parts of the CF potentials [6] in order to obtain a reasonable description of experimental data. Such a result has not previously been obtained in any CC analysis of polarized ^{6}Li scattering with potentials derived by the CF method.

The analysis confirmed some of the conclusions of the lower energy data analysis performed by means of the CDCC method with DF potentials [7]. The effect of the nonresonant $\alpha + d$ states of ^{6}Li on the differential cross section and first-rank TAP for ^{6}Li $+^{26}$Mg elastic scattering was considerable. The width of the continuum bins $\Delta k = 0.2$ fm^{-1} was sufficient for the present study. Calculations with the $\alpha + d$ states limited to the $L = 2$ resonant and $L = 0$ nonresonant states, however, have been found to differ significantly from the full calculations. The nonresonant states with $L = 1, 2$ played a very important role, especially for the second-rank TAP $^TT_{20}$.

The diagonal and coupling CF potentials were derived from $d +^{26}$Mg and $\alpha +^{26}$Mg potentials at bombarding energies of 20 and 40 MeV, respectively. Two sets of $\alpha +^{26}$Mg optical model potential parameters were examined [18], both giving very similar results. The $d +^{26}$Mg optical model potential parameters found previously in a global search [21] were used for the sake of comparison

with earlier studies at the lower energy of 44 MeV [5,6,8]. The analysis presented in [6] was devoted to the study of the anomalous renormalization of the CF potentials required to reproduce data for the elastic scattering differential cross section. It was found that the real part of the CF potential had to be reduced by about 40% even when the resonant and nonresonant $\alpha + d$ excited states of ^{6}Li were explicitly included in the calculations. Moreover, it was predicted that at higher incident energy no renormalization would be required for fits to scattering data. The present analysis confirms this prediction. The question of whether this result stems from the input parameters used cannot be answered since $\vec{d} + ^{26}$Mg scattering at 20 MeV bombarding energy has not been investigated. We noted, however, that calculations performed with other $d+^{26}$Mg optical model potential parameter sets found in a global analysis of polarized deuteron scattering from targets in the mass range $A = 27$–120, but at lower energies ($E_d = 9$–13 MeV) [20], also did not require any renormalization of the real part of CF potential. However, in order to obtain a similar description of the experimental data as shown in Figs. 3 and 4 the imaginary part of the CF potential had to be reduced by about 20%.

The spin-orbit potential for $d + ^{26}$Mg is the source of the CF spin-orbit potential for ^{6}Li $+^{26}$Mg scattering. In the present work two ^{6}Li-target spin-orbit potentials were tried, emerging consequently from the two d-target global optical model potentials [20,21]. The CF spin-orbit potential derived from the $d + ^{26}$Mg spin-orbit potential given in [21] was almost 10 times larger at the radii important for the scattering than the potential calculated from the parameters given in reference [20]. The CC calculations with this stronger potential gave a worse fit to the first-rank TAP for the elastic channel than the calculations plotted in Fig. 3, which were obtained with the weaker potential. The calculated angular distribution of iT_{11} had a shape similar to that shown in Fig. 3, but a larger amplitude. In both cases, however, the effect on the first-rank TAP due to the CF spin-orbit potential was dominated by *dynamic* effects caused by the projectile excitation. Thus, it is concluded that, as observed previously at ^{6}Li energies in the vicinity of the Coulomb barrier [2], the origin of the first-rank TAP observed for polarized ^{6}Li elastic scattering from ^{26}Mg is in the mechanism of the scattering rather than in the *static* CF spin-orbit potential.

The effect of coupling to nonresonant $\alpha + d$ excited states of ^{6}Li was also found to be of importance for the second-rank TAP $^TT_{20}$ for elastic scattering. Coupling to the three $L = 2$ resonant states alone resulted in a cancellation between the contributions from couplings to different excited states and the predicted values of $^TT_{20}$ were very small. The inclusion of couplings to the nonresonant continuum states produced substantial changes to the calculated angular distribution. These changes were enhanced by excitation of the target nucleus. Thus, the effects of the projectile and the target excitations are expected to compete with the effect caused by the *static* second-rank tensor potential for ^{6}Li $+^{26}$Mg. However, this competition could not be studied in the present work because of the lack of information on the $d + ^{26}$Mg second-rank tensor potential. Recently obtained experimental data of the first- and second-rank TAP's for polarized ^{6}Li scattering from ^{58}Ni at 70.5 MeV [24] offers an opportunity to investigate this competition in detail since $\vec{d} + ^{58}$Ni interactions at the relevant energy have been carefully investigated [25].

ACKNOWLEDGMENT

[1] I.J. Thompson and M.A. Nagarajan, Phys. Lett. **106B**, 163 (1981).

[2] H. Nishioka, R.C. Johnson, J.A. Tostevin, and K.-I. Kubo, Phys. Rev. Lett. **48**, 1795 (1982).

[3] Y. Sakuragi, M. Kamimura, M. Yahiro, and M. Tanifuji, Phys. Lett. **153B**, 372 (1985).

[4] H. Nishioka, J.A. Tostevin, R.C. Johnson, and K.-I. Kubo, Nucl. Phys. **A415**, 230 (1984).

[5] K. Rusek, J. Giroux, H.J. Jänsch, H. Vogt, K. Becker, K. Blatt, A. Gerlach, W. Korsch, H. Leucker, K. Luck, H. Reich, H.-G. Völk, and D. Fick, Nucl. Phys. **A503**, 223 (1989).

[6] Y. Hirabayashi and Y. Sakuragi, Phys. Lett. B **258**, 11 (1991).

[7] Y. Hirabayashi, Phys. Rev. C **44**, 1581 (1991).

[8] Y. Hirabayashi and Y. Sakuragi, Nucl. Phys. **A536**, 375 (1992).

[9] K. Rusek, H.J. Jänsch, K. Becker, K. Blatt, W. Korsch, H. Leucker, W. Luck, H. Reich, H.-G. Völk, and D. Fick, Phys. Lett. B **231**, 351 (1989).

[10] K. Becker, K. Blatt, H.J. Jänsch, W. Korsch, H. Leucker, W. Luck, H. Reich, H.-G. Völk, D. Fick, and K. Rusek, Nucl. Phys. **A535**, 189 (1991).

[11] R.P. Ward, N.M. Clarke, K.I. Pearce, C.N. Pinder, C.O. Blyth, H.D. Choi, P.R. Dee, S. Roman, G. Tungate, and N.J. Davis, Phys. Rev. C **50**, 918 (1994).

[12] I.J. Thompson, Comput. Phys. Rep. **7**, 167 (1988).

[13] J.E. Bowsher, T.B. Clegg, H.J. Karwowski, E.J. Ludwig, W.J. Thompson, and J.A. Tostevin, Phys. Rev. C **45**, 2824 (1992).

[14] Y. Sakuragi, Phys. Rev. C **35**, 2161 (1987).

[15] Y. Sakuragi, M. Yahiro, and M. Kamimura, Prog. Theor. Phys. **70**, 1047 (1983).

[16] K.-I. Kubo and M. Hirata, Nucl. Phys. **A187**, 186 (1972).

[17] F. Ajzenberg-Selove, Nucl. Phys. **A490**, 1 (1988).

[18] P.P. Singh, R.E. Malmin, M. High, and D.W. Devins, Phys. Rev. Lett. **23**, 1124 (1968).

[19] J. Nurzynski, T. Kihm, K.T. Knöpfle, G. Mairle, and H. Clement, Nucl. Phys. **A465**, 365 (1987).

[20] J.M. Lohr and W. Haeberli, Nucl. Phys. **A232**, 381 (1974).

[21] W.W. Daehnick, J.D. Childs, and Z. Vrcelj, Phys. Rev.

C **21**, 2253 (1980).

[22] H. Clement, R. Frick, G. Graw, P. Schiemenz, and N. Seichert, Z. Phys. A **314**, 49 (1983).

[23] P.W.F. Alons, H.P. Blok, J.F.A. Van Hienen, and J. Blok, Nucl. Phys. **A367**, 41 (1981).

[24] P.R. Dee, C.O. Blyth, N.M. Clarke, S.J. Hall, O. Karban, I. Martel-Bravo, S. Roman, K. Rusek, G. Tungate, R.P. Ward, N.J. Davis, K.A. Connell, and D.B. Steski, Phys. Rev. C (to be submitted).

[25] M. Takei, Y. Aoki, Y. Tagishi, and K. Yagi, Nucl. Phys. **A472**, 41 (1987).